Int. J. Heat Mass Transfer. Vol. 6, pp. 129–141. Pergamon Press 1963. Printed in Great Britain.

TRANSIENT HEAT DISSIPATION FROM STORAGE RESERVOIRS

Z. ROTEM, J. GILDOR and A. SOLAN

Department of Mechanical Engineering, Israel Institute of Technology, Haifa*

Abstract—An analysis of the transient behaviour of internally heated reservoirs or buildings is presented. New solutions for simplified geometrical models, which take account of both fluid heat capacity and convection resistance at the walls, are derived as a significant step towards the solution of the more general problem. The geometrical models considered are: the plane semi-infinite wall in contact with a well-mixed fluid and the spherical cavity in an infinite solid. Solutions are presented for both time dependent and time independent heat input rates.

Generally valid graphs and tables for the plane wall case with constant heat input rate are given.

NOMENCLATURE

a, H/K;
A, constant;
$\mathscr{A}$, function defined in equation (I-17);
B, constant;
c, specific heat of solid;
c_f, specific heat of fluid;
e, base of Naperian logarithms;
H, film convection coefficient;
i, integration operator for complementary error functions;
j, root of (-1);
K, thermal conductivity;
m, summation index;
M, mass of fluid in contact with unit wall area;
n, index; half integer greater than $(-\frac{1}{2})$;
p, Laplace transformation parameter;
q, $\sqrt{(p/\kappa)}$;
Q, heat input function;
r, radius;
R, radius of boundary of spherical cavity;
s, $(\rho c)_{\text{wall}}/Mc_f$;
S, s/a;
t, time;
t_c, critical time, defined in equation (22);
u, fluid temperature;
u_0, initial fluid temperature;
U, function defined in equation (11);
v, solid temperature;
v_0, initial solid temperature;
V, function defined in equation (11);
V_0, initial temperature of system;
x, length co-ordinate perpendicular to boundary;
z, complex variable;
$\bar{z}$, conjugate complex variable.

The superscript dash signifies transformed functions, except for $\bar{z}$.

Greek symbols

Γ, gamma function;
$\delta_{\mu\nu}$, Kronecker's delta;
ζ, variable, equation (II-1);
η, dimensionless root of equation, see (4) and (18);
η', root of equation, see (4) and (18);
θ, variable, equation (II-2);
κ, thermal diffusivity of solid;
λ, variable, equation (II-2);
Λ_n, constant of dimensions T^{-n};
μ, summation index;
ν, summation index;
ξ, variable;
ρ, density of solid;
τ, dimensionless time $= s^2\kappa t$;
τ^*, dimensionless time $= a^2\kappa t$;
ϕ, temperature function, equal to $v \cdot r$.

1. INTRODUCTION

1.1 *The problem*

TRANSIENT behaviour of internally heated storage reservoirs or of buildings upon heating up is of wide interest in technological applications. The great complication of the problem in its most

* This paper is in part based on an M.Sc. thesis of one of us (J.G.) submitted in 1960 at this Institute.

general statement has led to the consideration of simplified models amenable to analysis. The reservoir is usually considered to be of regular shape, filled with a hypothetical fluid, the heat capacity of which represents that of the contents. This fluid is usually assumed to be well mixed, i.e. the temperature differences within the fluid are neglected. The reservoir contains a heat source, the output of which may be time dependent or time independent, and heat is lost from the fluid through convection at the walls of the enclosure.

Although this system is idealized as compared with actual conditions, it is thought that the analysis of such a model forms a useful step towards predicting temperature variation in practice.

Thus the temperature variation with time of the system must depend on the heat input, the thermal capacity of the fluid, the convection resistance at the walls and the shape of the enclosure.

1.2. *Previous work on the subject*

Carslaw and Jaeger [1] investigated this problem, simplifying the geometrical configuration of the enclosure further. They considered the case for cylindrical (p. 344) and spherical (p. 349) cavities in an *infinite* solid medium, and presented the solutions in terms of non-tabulated integrals. For the spherical cavity the possibility of obtaining solutions explicitly in terms of complementary error functions is mentioned. The latter method, which leads to complex arguments for these functions in many cases of practical importance, is not elaborated. The cavity bounded by *plane* walls was also considered, but only for simplified cases when either fluid heat capacity, the film resistance or heat input were neglected ([1], p. 306–7). As corner effects were not taken account of, this last configuration is equivalent to a plane semi-infinite wall in contact with a well-stirred fluid.

Wolfe [2] considered a cavity formed by plane walls of *finite* thickness, again neglecting corner effects, and stipulating a constant rate of heat input. His solution leads to non-orthogonal eigenfunctions, and the computational effort involved in the calculation of practical cases is extensive indeed.

1.3. *Outline of main results*

It will be shown in the present work that the simplification of the model to infinitely thick enclosures does not lead to great errors in temperatures predicted, in most technological applications.* On the other hand, neglecting either fluid heat capacity or contact resistance at the walls is often not admissible. The present work presents *explicit* solutions for the plane semi-infinite wall and for the spherical cavity in an infinite solid, taking account of both fluid heat capacity *and* convection resistance, and for heat input rates which may or may not depend on time. These solutions are more general than those of references [1] and [2], while also leading to a great simplification in the computational work involved, compared to [2].

The solutions, apparently not hitherto published, are obtained in terms of recently tabulated functions [3]. In another paper [4] test results on a thick-walled room under transient conditions are described, and the applicability of the theoretical model predictions is established.

2. MATHEMATICAL ANALYSIS

2.1. *Solution for cavity bounded by plane walls*

Consider a cavity bounded by plane walls of surface area equal to that of the room, filled with a well-mixed hypothetical fluid the heat capacity of which is equal to that of the contents of the room. Considering the time scale of temperature variation in technologically significant cases, equalization of temperature within the fluid, either by natural convection or (the more usual case) by forced mixing, is sufficiently rapid for the well-mixed-fluid simplification to be admissible.

All physical properties are considered constant. Neglecting corner effects this model amounts to the consideration of a plane semi-infinite wall in contact with a well-mixed fluid. The heat conduction equation for this case is,

$$\frac{\partial^2 v}{\partial x^2} - \frac{1}{\kappa}\frac{\partial v}{\partial t} = 0, \qquad t > 0; \quad x \geqslant 0 \quad (1)$$

* For deep underground reservoirs the solution is exact.

and the boundary conditions are:

$$\left.\begin{aligned} &t=0; \qquad u=v=V_0 \\ &t>0;\ x=0;\ K\frac{\partial v}{\partial x}+H(u-v)=0 \\ &x=0;\ Mc_f\frac{\mathrm{d}u}{\mathrm{d}t}+H(u-v)=Q(t). \end{aligned}\right\} \quad (2)^*$$

Here v is enclosure temperature, u is fluid temperature, K is enclosure thermal conductivity, H the film coefficient at the enclosure walls, M is the mass of fluid in contact with unit wall area and c_f is fluid specific heat. V_0 is put equal to zero arbitrarily in what follows.

2.2. *The heat input function*

Heat is supplied to the fluid at a rate $Q(t)$, which is a function of time. The simplest function will be $Q(t)=\Lambda_n t^n$ per unit time and per unit wall area, where Λ_n is a constant. More general functions may be represented by a series of such terms, and the solutions to be derived here may be superposed, due to the linear nature of equation (1). For analytical reasons, n must be an integer or a half integer greater than $(-\frac{1}{2})$.

In practical applications, heating by steam coil at approximately constant steam temperature will give rise to "equivalent" exponents n smaller than zero. This, as with a rise in fluid temperature heat output is reduced. On the other hand, if the steam is supplied from a boiler during the starting up period, or if an electrical heating method is used, n may be zero or larger.

Applying the Laplace transformation [5] to (1) and (2) the following result for the transformed temperature $\bar{v}$ is obtained (see Appendix I-a):

$$\bar{v}=\frac{ase^{-qx}}{Kpq(q^2+aq+as)}\cdot\frac{\Lambda_n\Gamma(n+1)}{p^n} \quad (3)$$

where the parameters $a=H/K$; $s=(\rho c)_{\text{wall}}/Mc_f$ both have the dimension of $|L|^{-1}$. p is the Laplace transformation parameter, and $q=\sqrt{(p/\kappa)}$. Γ is the gamma function.

* The initial temperatures u_0, v_0, respectively V_0, may be put equal to zero arbitrarily. In case the temperatures u_0 and v_0 are different, a more general solution may be obtained by superposition of [1], p. 307, case (iii) on the solutions given here.

The inversion of $\bar{v}$ will be performed by splitting (3) into partial fractions.

2.3. *Investigation of the roots of the denominator polynomial of equation* (3)

The two roots with reversed algebraical signs will be given by

$$\eta_1=\frac{\eta_1'}{a}=\tfrac{1}{2}-\sqrt{(\tfrac{1}{4}-S)},$$

$$\eta_2=\frac{\eta_2'}{a}=\tfrac{1}{2}+\sqrt{(\tfrac{1}{4}-S)} \quad (4)$$

where S is the dimensionless ratio s/a.

In case the roots are different (real or complex), then

$$\bar{v}=\frac{ase^{-qx}}{Kpq(\eta_2'-\eta_1')}\left(\frac{1}{q+\eta_1'}-\frac{1}{q+\eta_2'}\right)\frac{\Lambda_n\Gamma(n+1)}{p^n}. \quad (5)$$

It is shown in the appendix (I-b) that the inversion of $\bar{v}$ gives the following result for the enclosure temperature:

$$v=\frac{as\Lambda_n\Gamma(n+1)}{\kappa^n K(\eta_1'-\eta_2')}\sum_{\nu=1}^{2}(-1)^\nu\frac{1}{(-\eta_\nu')^{2n+2}}\left\{e^{\eta_\nu' x+\kappa t(\eta_\nu')^2}\cdot\operatorname{erfc}\left[\frac{x}{2\sqrt{(\kappa t)}}+\eta_\nu'\sqrt{(\kappa t)}\right]-\sum_{m=0}^{2n+1}\left[[-2\eta_\nu'\sqrt{(\kappa t)}]^m i^m\operatorname{erfc}\frac{x}{2\sqrt{(\kappa t)}}\right]\right\}. \quad (6)$$

This result may now be differentiated and inserted into the second of the boundary conditions (2) to give an expression for fluid temperature in dimensionless form:

$$u\frac{(s^2\kappa)^n Ks}{\Lambda_n}=\frac{a\Gamma(n+1)}{(\eta_1'-\eta_2')}\sum_{\nu=1}^{2}(-1)^\nu\left(-\frac{s}{\eta_\nu'}\right)^{2(n+1)}\left\{\left(1-\frac{\eta_\nu'}{a}\right)e^{\kappa t(\eta_\nu')^2}\cdot\operatorname{erfc}[\eta_\nu'\sqrt{(\kappa t)}]-1-\sum_{m=1}^{2n+1}\left[[-\eta_\nu'\sqrt{(\kappa t)}]^m\left(\frac{1}{\Gamma[(m/2)+1]}+\frac{1}{a\sqrt{(\kappa t)}}\cdot\frac{1}{\Gamma[(m+1)/2]}\right)\right]\right\}. \quad (7)$$

For the special case when the heat input rate is constant, i.e. $n = 0$,

$$Q = A_0 t^0 = A_0 = \text{constant}$$

and from (7)

$$u\frac{Ks}{A_0} = \frac{2}{\sqrt{\pi}} S(\tau^*)^{1/2} - 1 + S + \frac{1}{\eta_2 - \eta_1} \{\eta_2^3 e^{\eta_1^2 \tau^*} \operatorname{erfc}[\eta_1(\tau^*)^{1/2}] - \eta_1^3 e^{\eta_2^2 \tau^*} \operatorname{erfc}[\eta_2(\tau^*)^{1/2}]\} \quad (8)$$

where the dimensionless time $\tau^* = a^2 \kappa t$ and $\eta_1 \cdot \eta_2 = S$.

Computational results of this equation of an accuracy and range which should cover most applications are given in Table 1.

It is often more convenient to use a different dimensionless group:

$$\frac{uH}{A_0} = \frac{2}{\sqrt{\pi}} (\tau^*)^{1/2} + 1 - \frac{1}{S} + \frac{1}{S} \cdot \frac{1}{\eta_2 - \eta_1} \left\{ \tfrac{3}{2} e^{\eta_1^2 \tau^*} \operatorname{erfc}[\eta_1(\tau^*)^{1/2}] - \eta_1^3 2^2 \tau^* \operatorname{erfc}[\eta_2(\tau^*)^{1/2}] \right\}. \quad (9)$$

Equation (9) is more convenient than (8) for graphical representation of many cases of practical importance. Plots are given in Fig. 2.

It may be remarked that by superposition of solutions (7) for various n, fluid temperature for any analytical heat input function may now be calculated, with desk calculators as sole computational aid.

Further, for very large dimensionless times, the solution above asymptotically approaches

$$\frac{uH}{A_0} \to \frac{2}{\sqrt{\pi}} (\tau^*)^{1/2} + 1 - \frac{1}{S}. \quad (10)$$

Thus, a steady state is not approached.

Investigation of the solutions (6) *and* (7) *for various kinds of roots*

(α) *Both roots real.* This implies $S < \frac{1}{4}$. The values of the error function may be taken from standard tables and computed results may be obtained from the equations.

(β) *Both roots complex.* This implies $S > \frac{1}{4}$. Tables for $e^{-z^2} \cdot \operatorname{erfc}(z)$ have recently been published [3]. However, the form in which these

Table 1. uKs/A_0 as a function of τ for various S. Case of plane semi-infinite wall

τ	$\frac{uKs}{A_0}$	τ	$\frac{uKs}{A_0}$
(a) $H = \infty$, $S = 0$			
0	0	1·440	0·733
0·0004	0·000394	1·690	0·825
0·0016	0·001553	1·960	0·918
0·0036	0·003444	2·250	1·014
0·0064	0·006034	2·560	1·111
0·0100	0·009295	2·890	1·210
0·0144	0·013197	3·24	1·310
0·0256	0·02282	3·61	1·399
0·0400	0·03470	4·00	1·492
0·0576	0·04865	4·84	1·70
0·0784	0·06452	5·76	1·91
0·1024	0·08214	6·76	2·12
0·1296	0·1014	7·84	2·34
0·1600	0·1221	9·00	2·56
0·1936	0·1443	10·24	2·78
0·2304	0·1677	11·56	3·00
0·2704	0·1923	12·96	3·21
0·3136	0·2181	14·44	3·43
0·3600	0·2448	16·00	3·65
0·4356	0·2868	17·64	3·87
0·5184	0·3306	19·36	4·09
0·6084	0·3762	21·16	4·31
0·7056	0·4234	23·04	4·53
0·8100	0·4721	25·0	4·75
1·000	0·5560	49·0	6·98
1·210	0·643	100·0	10·34
(b) $S = 0·2$			
0	0	0·33511	0·25598
0·001885	0·001877	0·42412	0·31115
0·003350	0·003331	0·5236	0·36921
0·005236	0·005181	0·7540	0·49241
0·016965	0·016465	1·0263	0·62301
0·03540	0·03350	1·3404	0·75942
0·06053	0·05559	1·6965	0·90017
0·09236	0·08239	1·9102	0·97902
0·13092	0·11307	3·6493	1·54781
0·18850	0·15630	7·6407	2·43761
0·25676	0·20417		
(c) $S = 1/4$			
0	0	1·00	0·6235
0·0484	0·0453	1·44	0·8154
0·0676	0·0622	2·25	1·1165
0·0900	0·0813	2·89	1·3245
0·2025	0·1691	4·00	1·641
0·2500	0·2031	6·25	2·180
0·3600	0·2774	12·25	3·277
0·4900	0·3571	25·00	4·932
0·640	0·442		

Table 1.—continued

τ	$\frac{uKs}{\Lambda_0}$	τ	$\frac{uKs}{\Lambda_0}$
(d) $S = 1/3$			
0	0	0·691	0·484
0·00853	0·00841	0·941	0·618
0·01333	0·01309	1·333	0·795
0·01920	0·01876	1·920	1·031
0·02615	0·02535	2·613	1·273
0·03413	0·03285	3·413	1·519
0·04320	0·04120	4·320	1·769
0·05333	0·04789	6·453	2·276
0·07679	0·07125	7·680	2·528
0·1045	0·09498	9·013	2·783
0·1728	0·15096	10·453	3·040
0·2581	0·21396	20·144	4·444
0·3605	0·28470		
(e) $S = 1$			
0	0	1·6132	1·0805
0·00853	0·00848	1·9199	1·2243
0·01333	0·01324	2·2533	1·3687
0·01920	0·01906	2·6131	1·5132
0·02615	0·02571	3·0000	1·6574
0·03413	0·03364	3·4132	1·8010
0·04320	0·04241	3·853	1·981
0·05333	0·05212	4·320	2·087
0·07679	0·07427	5·333	2·370
0·10453	0·10016	6·453	2·650
0·13652	0·12933	7·680	2·927
0·1728	0·1615	9·013	3·202
0·2133	0·1977	10·453	3·475
0·2581	0·2344	11·999	3·747
0·3072	0·2749	13·653	4·017
0·3605	0·3171	15·413	4·287
0·4181	0·3618	17·279	4·554
0·4800	0·4086	19·077	4·823
0·5808	0·4810	21·332	5·090
0·6912	0·5570	23·519	5·356
0·8321	0·6352	25·812	5·622
0·9407	0·7159	28·212	5·887
1·0799	0·7983	30·718	6·152
1·3333	0·9380	33·331	6·417
(f) $S = 8$			
0	0	8·258	5·603
0·08258	0·08221	16·186	8·411
0·16186	0·16063	33·032	11·638
0·47557	0·46176	74·33	15·66
1·32128	1·26270	206·5	22·6
4·0464	3·2794		

functions are given needs some modification for our purposes, (see Appendix II).

For convenience, the arguments are henceforth applied to the case of constant heat input only. The solution (9) may be written:

$$\frac{uH}{\Lambda_0} = \frac{2}{\sqrt{\pi}}(\tau^*)^{1/2} + 1 - \frac{1}{S} - \left(1 - \frac{1}{S}\right) U[\sqrt{(S - \tfrac{1}{4})} \,.\, (\tau^*)^{1/2}; \tfrac{1}{2}(\tau^*)^{1/2}] - \frac{3 - 1/S}{2\sqrt{(S - \tfrac{1}{4})}} V[\sqrt{(S - \tfrac{1}{4})} \,.\, (\tau^*)^{1/2}; \tfrac{1}{2}(\tau^*)^{1/2}] \tag{11}$$

where U and V are functions explained in Appendix II.

(γ) *Both roots equal and real*, i.e. $S = \frac{1}{4}$. From (3) we now have

$$\bar{v} = \frac{ase^{-qx}}{Kpq(q + a/2)^2} \cdot \frac{\Lambda_n \Gamma(n+1)}{p^n}. \tag{12}$$

Proceeding as outlined above, the enclosure temperature may be found (Appendix I-c). We restrict ourselves here to giving the result for $n = 0$ only:

$$v = \frac{as\Lambda_0}{(\eta')^2 K}\left\{4\left(\frac{\kappa t}{\pi}\right)^{1/2} e^{-x^2/4\kappa t} - \left(\frac{2}{\eta'} + x\right) \operatorname{erfc} \frac{x}{2\sqrt{(\kappa t)}} + \left(\frac{2}{\eta'} - x - 2\kappa t\eta'\right) e^{\eta' x + \kappa t(\eta')^2} \,.\, \operatorname{erfc}\left[\frac{x}{2\sqrt{(\kappa t)}} + \eta'\sqrt{(\kappa t)}\right]\right\}; \qquad \eta' = \frac{a}{2}. \tag{13}$$

Fluid temperature is derived again as before:

$$\frac{uH}{\Lambda_0} = \frac{3}{\sqrt{\pi}}(\tau^*)^{1/2} - 3 + \left(3 - \frac{\tau^*}{2}\right) e^{\tau^*/4} \,.\, \operatorname{erfc} \frac{\sqrt{\tau^*}}{2}. \tag{14}$$

Now it can be seen that for all solutions, the dimensionless function uH/Λ_0 depends on the dimensionless characteristic time τ^* and on the parameter S only.

Asymptotic solutions (limiting cases)

Limiting cases of $S = 0$ may correspond to either (a) an infinitely great total fluid heat

capacity ($s = 0$), or (b) zero film heat convection resistance ($a = \infty$). At the other extreme $S = \infty$ may be obtained with either (c) no fluid heat capacity ($s = \infty$), or (d) infinite convection heat transfer resistance ($a = 0$).

The asymptotic solutions are examined in Appendix III-a. They lead to known classical results.

2.4. *Solution for the cavity of spherical shape*

Equation (1) and boundary conditions (2) take the following form:

$$\frac{\partial v}{\partial t} = \kappa\left(\frac{\partial^2 v}{\partial r^2} + \frac{2}{r}\frac{\partial v}{\partial r}\right) \tag{15}$$

$$\left.\begin{aligned} &t = 0 && u = v = V_0 = 0 \\ &t > 0;\ r = R; && K\frac{\partial v}{\partial r} + H(u - v) = 0 \\ &r = R; && Mc_f\frac{\mathrm{d}u}{\mathrm{d}t} + H(u - v) = \Lambda_n t^n \\ &r \to \infty; && v \text{ to remain finite.} \end{aligned}\right\} \tag{16}$$

The transformation $\phi = vr$ brings (15) back to the form of (1).

Using operational calculus on the transformed equation yields a result for enclosure temperature (Appendix I-d):

$$v = -\frac{a^2 RS\Lambda_n \Gamma(n+1)}{H\kappa^n(\eta_1-\eta_2)(\eta_2-\eta_3)(\eta_3-\eta_1)}\cdot\frac{1}{r}\cdot\sum_{\nu=1}^{3}\left\{\frac{\delta_{1\nu}(\eta_2-\eta_3)+\delta_{2\nu}(\eta_3-\eta_1)+\delta_{3\nu}(\eta_1-\eta_2)}{(-\eta_\nu)^{2n+1}}\right.$$
$$\cdot\left\{e^{\eta_\nu(r-R)+\kappa\eta_\nu^2 t}\operatorname{erfc}\left[\frac{r-R}{2\sqrt{(\kappa t)}}+\eta_\nu\sqrt{(\kappa t)}\right]\right.$$
$$\left.\left.-\sum_{m=0}^{2n}\left[[-2\eta_\nu\sqrt{(\kappa t)}]^m i^m\operatorname{erfc}\frac{r-R}{2\sqrt{(\kappa t)}}\right]\right\}\right\} \tag{17}$$

where η_ν are the roots of the cubic equation (with reversed algebraical sign),

$$q^3 + (a + 1/R)q^2 + asq + as/R = 0 \tag{18}$$

and $\delta_{\mu\nu}$ is Kronecker's delta. Similarly, fluid temperature is given by,

$$u = -\frac{a^2 s\Lambda_n\Gamma(n+1)}{H\kappa^n(\eta_1-\eta_2)(\eta_2-\eta_3)(\eta_3-\eta_1)}\cdot\sum_{\nu=1}^{3}\left\{\frac{\delta_{1\nu}(\eta_2-\eta_3)+\delta_{2\nu}(\eta_3-\eta_1)+\delta_{3\nu}(\eta_1-\eta_2)}{(-\eta_\nu)^{2n+1}}\right.$$
$$\cdot\left\{\left(1+\frac{1}{aR}-\eta_\nu/a\right)e^{\kappa\eta_\nu^2 t}\operatorname{erfc}\left[\eta_\nu\sqrt{(\kappa t)}\right]\right.$$
$$+\frac{1/a}{\sqrt{(\pi\kappa t)}}-\sum_{m=0}^{2n}[-\eta_\nu\sqrt{(\kappa t)}]^m$$
$$\left.\left.\cdot\left[\frac{1+1/aR}{\Gamma[(m/2)+1]}+\frac{1/a}{\sqrt{(\kappa t)}\Gamma[(m+1)/2]}\right]\right\}\right\}. \tag{19}$$

For constant heat input, i.e. $n = 0$, equation (19) reduces to

$$\frac{Ku}{\Lambda_0 R} = \frac{s/R^2}{(\eta_1-\eta_2)(\eta_2-\eta_3)(\eta_3-\eta_1)}\cdot\sum_{\nu=1}^{3}\left\{\frac{\delta_{1\nu}(\eta_2-\eta_3)+\delta_{2\nu}(\eta_3-\eta_1)+\delta_{3\nu}(\eta_1-\eta_2)}{\eta_\nu}\right.$$
$$\left.\cdot[(1+aR-R\eta_\nu)e^{\kappa\eta_\nu^2 t}\operatorname{erfc}[\eta_\nu\sqrt{(\kappa t)}]-(1+aR)]\right\}. \tag{20}$$

For constant heat input ($n = 0$), the limit when $t \to \infty$ is,

$$\frac{uK}{\Lambda_0 R} = 1 + \frac{1}{aR} \tag{21}$$

i.e. steady state is approached, as time increases.

Equations (17–20) have been investigated in the manner of (6–9) for the various kinds of roots of (18), viz.

- (α) All roots η_ν real and different.
- (β) Two roots conjugate complex, one root real.
- (γ) All roots real, two roots identical.
- (δ) All roots real and identical.

The investigation is rather cumbersome and will not be described here.* Again, (β) leads to com-

* Interested readers may obtain the details of the derivations from one of the authors (Z.R.).

plementary error functions with complex arguments.

Limiting cases were again investigated as before and results are given in Appendix III-b.

3. GRAPHICAL REPRESENTATION

Inspection of all equations giving solutions for v and u for the plane-wall case will reveal two alternative methods of plotting, both having n as a parameter of the whole plot:

(a) $\dfrac{uKs}{\Lambda_n/(s^2\kappa)^n}$ versus τ, with S as a parameter;

or

(b) $\dfrac{uH}{\Lambda_n/(s^2\kappa)^n}$ versus τ^* with S as a parameter.

All these groups are dimensionless variables. For the exponent $n = 0$, method (a) will be more useful for those cases where s is not expected to approach the extreme values of zero or infinity, while the second method is suitable provided a does not approach those limits. Figs. (1) and (2) give such plots for the plane-wall case, with constant heat input. Table 1 gives numerical data for this case.

In practical cases the value of the parameter S will be within the range of 10–500 for air enclosed in concrete walls, while for water S will be rather less than $\frac{1}{4}$.* Thus it is seen that for all practical heating and ventilating applications the solutions with complex roots will be applicable. As an example, for air at atmospheric pressure and temperature, of an equivalent thickness of 3 m in contact with any wall, with $H = 15$ kcal/(m² degC h), and walls of standard concrete, S will be equal to 30.

A repetition of the same argument for the case of the spherical cavity leads to the conclusion that here the dimensionless groups are, for any constant exponent n, the same as those given above. However, an extra parameter equal to aR also appears. It is, therefore, impractical to show general plots valid for all values of aR.

4. DISCUSSION

4.1. *Demonstration of the accuracy of the method when applied to finite walls*

The case calculated by Wolfe [2] related to air contained by concrete walls only 8 in thick, and to constant heat input. Table 2 gives a comparison of Wolfe's data and those calculated from (11).

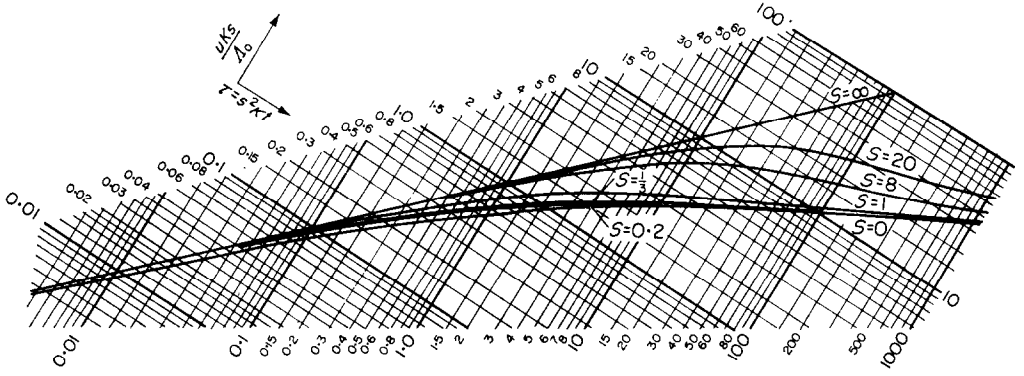

FIG. 1. Dependence of uKs/Λ_0 on $\tau = s^2\kappa t$.

Thus, it is seen that for periods shorter than 20 h, the error caused by assuming the walls infinitely thick is smaller than 2·5 per cent.

A similar result was obtained from tests [4].

4.2. *Comparison between the plane infinite-wall model and the spherical cavity model as applied to a cubical room*

This comparison was carried out for a cubical room containing air at atmospheric pressure and temperature, with $H = 3$ kcal/(m² degC h),

* An exception to this is the case when the fluid is enclosed in a metal container buried in the soil: the contact resistance is here determined by the heat transfer between the outer metal envelope and the soil, and may be rather high. Thus S will be large.

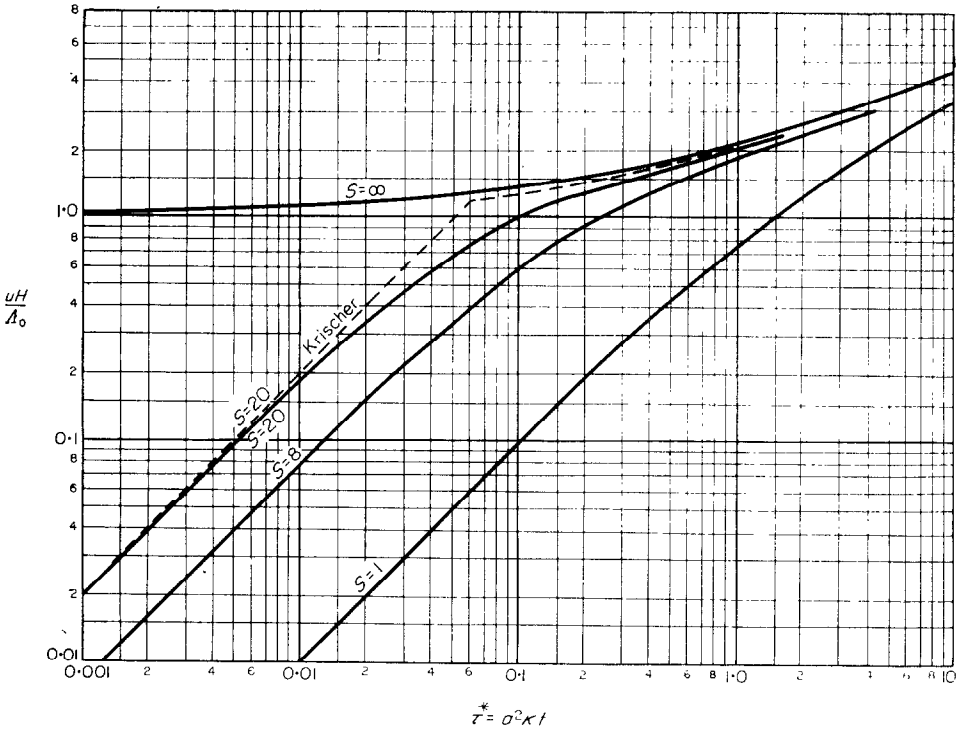

FIG. 2. Dependence of uH/Λ_0 on $\tau^* = a^2\kappa t$.

$S = 260$, and constant heat input. The comparison was carried out for equivalent envelope area. Table 3 gives the results.

In actual practice, a room of doubly rectangular cross section is, of course, much better represented by the geometrical model of a sphere than that of plane walls with no corner effects [6, 7]. But from Table 3 it is clear that for short times the graphical plots given for the plane-wall model may be used for practical configurations, with small errors only.

Table 2. Comparison of Wolfe's data with results obtained through equation (11)

Time (h)	5	10	20	30	40	50	70
u/Λ_0 Wolfe	0·95	1·14	1·405	1·583	1·69	1·74	1·81
u/Λ_0 equation (11)	0·969	1·165	1·44	1·647	1·83	1·98	2·25
Difference (per cent)	1·97	2·1	2·5	4·1	8·3	13·9	24·3

Table 3. Comparison of plane-wall model to spherical cavity model for a cubical room, large S

Equivalent radius (m)	Time to reach 99·5 per cent steady state temperature for sphere (years)	Time for difference in u/Λ_0 between the two models not exceeding 3·15 per cent (h)	Time for difference not exceeding 15 per cent (h)
6·91	300	100	1000
2·00	24·5	8·16	81·6
0·50	1·5	0·51	5·1

4.3. *Other approximate solutions*

Krischer [8] has proposed an approximate calculation method assuming that initially there is no heat dissipation to the walls, while from a

certain critical time onwards, all heat input is dissipated through wall conduction. The critical time is given by

$$t_c = \frac{Mc_f}{H}. \tag{22}$$

With t_c assumed as zero datum, wall temperature thereafter is calculated as for the constant flux case ([1], p. 75).

The temperature variation according to Krischer, for $S = 20$, is also plotted in Fig. 2. As would be expected the greatest error, compared to the exact solution, is obtained around the critical time.

Another approximate method used for heating and ventilating purposes is to neglect air heat capacity. The errors of both Krischer's method and this latter assumption are compared to the exact solution for infinitely thick walls in Fig. 3. The maximum error of Krischer's method is seen to be at $\tau^* = 0{\cdot}05$: this corresponds to about 5 min for a practical case considered. Even after 15 min the discrepancy is still 15 per cent.

5. CONCLUSIONS

Solutions for two models representing a room containing a heat source with time dependent output, filled with a well-mixed fluid of finite heat capacity are given. Heat is dissipated to the walls with finite film heat-transfer resistance.

The two models considered are: the plane, infinitely thick wall and the spherical cavity in an infinite solid. All physical properties were assumed constant.

It is shown, that in most practical cases arising in air-conditioning technology, the problem leads to solutions expressed in terms of error functions with a complex argument. In some cases of storage reservoir technology the arguments will be real.

These solutions, which to the best of our knowledge have not been previously published, represent generalizations of well known partial solutions for semi-infinite solids.

Wolfe [2] considered a model closer to real conditions in one respect: with his model the cavity was bounded by plane walls of *finite* thickness, with heat convection on the outside taken into consideration also. This was done for constant heat input rate only, and neglecting corner effects.

The results given here are much simpler than those obtained by Wolfe, and moreover lend

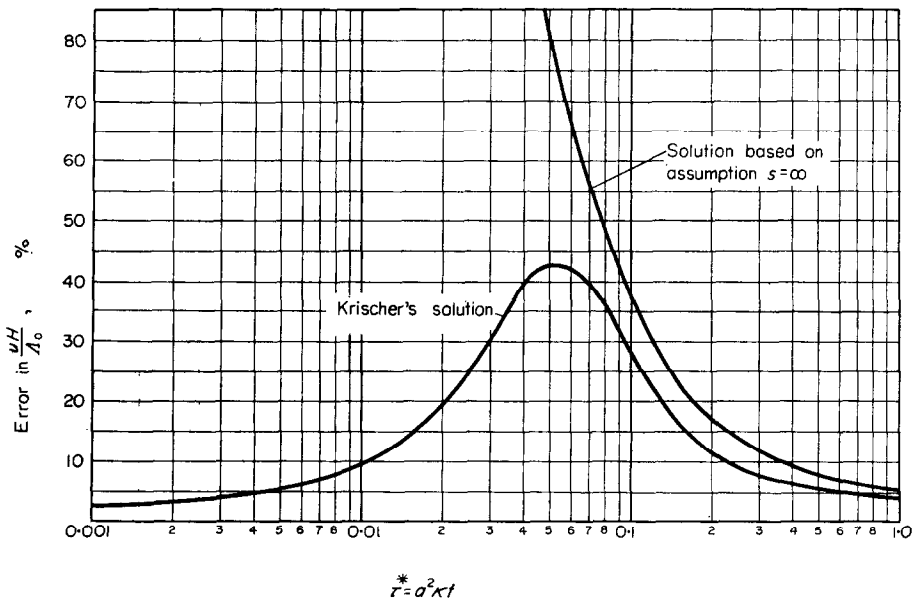

FIG. 3. Deviation of two approximate solutions from the exact semi-infinite wall solution ($S = 20$).

themselves to generalization for non-constant heat input. Also, solutions were derived for the spherical model which, for thick walls (where corner effects are significant) should give results more accurate than those for the plane wall.

Table 2 shows that the solutions here given are of adequate accuracy even for the practical configuration considered by Wolfe. In an engineering context, the possibility of giving the general solution in a graphical plot must be considered an important advantage.

The assumption of simpler models in engineering usage, such as neglecting fluid heat capacity, or the Krischer assumption can, on occasion, lead to considerable error, especially when applied to the design of a heated reservoir (small S). Estimates of the error for a case of air conditioning is given in Fig. 3.

It is interesting to note that the model employing infinitely thick plane walls will not tend asymptotically towards steady state as time goes on (at constant heat input). Here, again, the spherical model is qualitatively closer to actual conditions in that for constant heat input it does tend towards steady state.

Lastly, it is seen that for any given configuration and for all cases of heat input function discussed here, U/A_n is a unique function of dimensionless time.

REFERENCES

1. H. S. CARSLAW and J. C. JAEGER, *Conduction of Heat in Solids* (2nd Ed.). Oxford University Press, London (1959).
2. W. A. WOLFE, Transient response of heated air in an enclosure with heat losses, *Trans. ASME* C **81**, 19–23 (1959).
3. F. A. FADDEEVA and N. M. TERENT'EV, *Tables of the Values of the Probability Integral of a Complex Argument*. State Publishing House of Technical-Theoretical Literature, Moscow (1954). (In Russian).
4. J. GILDOR, Z. ROTEM and A. SOLAN, Transient temperature response of a test room filled with well-mixed fluid of finite heat capacity. Bull. Res. Coun. Israel 11 G (1962).
5. H. C. CARSLAW and J. C. JAEGER, *Operational Methods in Applied Mathematics* (2nd Ed.). Oxford University Press, London (1948).
6. U.S. Nat. Bur. of Standards, Technical Report No. 2122, October (1957).
7. G. LORENTZEN, The design and performance of an un-insulated freezer room in rock, Proc. 10th Int. Congr. Refrig. Pergamon Press, London (1959).
8. O. KRISCHER and W. KAST, Zur Frage des Wärmebedarfs beim Anheizen selten beheizter Gebäude. *Ges. Ing.* **78**, 321–352 (1957).

APPENDIX 1

(a) *Derivation of equation* (3)

Applying the Laplace transformation to (1) and (2):

$$\frac{\mathrm{d}^2\bar{v}}{\mathrm{d}x^2} - \frac{p}{\kappa}\bar{v} + \frac{v_0}{\kappa} = 0 \qquad \text{(I-1)}$$

$$t > 0\ ;\ x = 0\ ;\ K\,\mathrm{d}\bar{v}/\mathrm{d}x + H(\bar{u} - \bar{v}) = 0 \qquad \text{(I-2)}$$

$$x = 0\ ;\ Mc_f(p\bar{u} - u_0) + H(\bar{u} - \bar{v}) = A_n\frac{\Gamma(n+1)}{p^{n+\frac{1}{2}}}. \qquad \text{(I-3)}$$

In what follows V_0 is put equal to zero arbitrarily. Eliminating $\bar{u}$ between (I-2) and (I-3),

$$\left(1 + \frac{Mc_f p}{H}\right)\cdot\frac{\mathrm{d}\bar{v}}{\mathrm{d}x} - \frac{Mc_f p}{K}\bar{v} + \frac{A_n}{K}\cdot\frac{\Gamma(n+1)}{p^{n+\frac{1}{2}}} = 0 \qquad n > -\tfrac{1}{2}\ ;\ x = 0\,. \qquad \text{(I-4)}$$

The solution of equation (I-1) taking (2) into account, is

$$\bar{v} = Ae^{-qx} + Be^{+qx} \qquad q \neq 0 \qquad \text{(I-5)}$$

where $q^2 = p/\kappa$; as the temperature has to be finite everywhere $B \equiv 0$.

Inserting (I-5) into (I-4) will furnish A: then the solution of (I-1) is given by (3).

(b) *Derivation of equation* (7)

The inverse Laplace transformation of

$$\frac{e^{-q.x}}{p^{n+1}q(q+\eta')}$$

gives

$$\frac{1}{\kappa^n(-\eta')^{2(n+1)}}\cdot\left\{e^{\eta' x+\kappa t(\eta')^2}\,\mathrm{erfc}\left(\frac{x}{2\sqrt{(\kappa t)}} + \eta'\sqrt{(\kappa t)}\right) - \sum_{m=0}^{2n+1}\left[[-2\eta'\sqrt{(\kappa t)}]^m \mathrm{i}^m\,\mathrm{erfc}\,\frac{x}{2\sqrt{(\kappa t)}}\right]\right\}. \qquad \text{(I-6)}$$

Inserting this into (5) and rearranging will furnish (6). This last equation may be differentiated, giving

$$\frac{\partial v}{\partial x} = \frac{as\Lambda_n\Gamma(n+1)}{\kappa^n K(\eta_1' - \eta_2')} \sum_{\nu=1}^{2} \frac{(-1)^\nu}{(-\eta_\nu')^{2n+2}} \left\{ \eta_\nu' e^{\eta_\nu' x + \kappa t(\eta_\nu')^2} \cdot \operatorname{erfc}\left(\frac{x}{2\sqrt{(\kappa t)}} + \eta_\nu' \sqrt{(\kappa t)} \right) + \frac{1}{2\sqrt{(\kappa t)}} \cdot \sum_{m=1}^{2n+1} \left[[-2\eta_\nu' \sqrt{(\kappa t)}]^m i^m i^{m-1} \operatorname{erfc} \frac{x}{2\sqrt{(\kappa t)}} \right] \right\}. \quad \text{(I-7)}$$

Inserting (6) and (I-7) into the second boundary condition (2) gives an expression for fluid temperature, (7).

(c) *Derivation of equation* (14)

The application of the inversion theorem to (12) may be simplified by differentiating (I-6) with respect to the parameter η'. Hence the inverse transformation of

$$\frac{e^{-qx}}{p^{n+1} q (q+\eta')^2}$$

is

$$-\frac{1}{\kappa^n} \cdot \frac{1}{(-\eta')^{2n+2}} \left\{ \left(-\frac{2(n+1)}{\eta'} + x + 2\kappa t \eta' \right) \cdot e^{\eta' x + \kappa t (\eta')^2} \cdot \operatorname{erfc}\left[\frac{x}{2\sqrt{(\kappa t)}} + \eta' \sqrt{(\kappa t)} \right] - 2\sqrt{(\kappa t/\pi)} \cdot e^{-x^2/4\kappa t} + \frac{1}{\eta'} \sum_{m=0}^{2n+1} [2(n+1) - m] \cdot \left[[-2\eta' \sqrt{(\kappa t)}]^m i^m \operatorname{erfc} \frac{x}{2\sqrt{(\kappa t)}} \right] \right\}. \quad \text{(I-8)}$$

The solution for v is again obtained by multiplying expression (I-8) by $[(as/K).\ \Lambda_n\Gamma(n+1)]$. It is convenient to discuss the properties of the solution on the simpler case of time independent heat input, i.e. for $n = 0$. This leads to equations (13) and (14).

(d) *Derivation of equation* (17)

The transformation $\phi = vr$ brings (15) back to the form of (1):

$$\frac{\partial \phi}{\partial t} - \kappa \frac{\partial^2 \phi}{\partial r} = 0 \quad \text{(I-9)}$$

with boundary conditions,

$$t = 0 \qquad \phi = u = 0 \quad \text{(I-10)}$$

$$t > 0; \quad r = R; \quad \frac{\partial \phi}{\partial r} = \phi(a + 1/R) - aRu \quad \text{(I-11)}$$

$$r = R; \quad Mc_f \frac{du}{dt} + H(u - \phi/R) = \Lambda_n t^n. \quad \text{(I-12)}$$

Applying the Laplace transformation to equations (I-9) through (I-12) yields:

$$t > 0; \ R \leqslant r < \infty; \quad \frac{d^2\bar{\phi}}{dr^2} - q^2\bar{\phi} + \frac{\phi_0}{\kappa} = 0 \quad \text{(I-13)}$$

$$\frac{d\bar{\phi}}{dr} = \bar{\phi}(a + 1/R) - aR\bar{u} \quad \text{(I-14)}$$

$$Mc_f(p\bar{u} - u_0) + H(\bar{u} - \bar{\phi}/R) = \Lambda_n\Gamma(n+1)/p^{n+1}. \quad \text{(I-15)}$$

The solution of these equations leads to

$$\bar{\phi} = \mathscr{A} e^{-qr} \quad \text{(I-16)}$$

where $\mathscr{A}$ is given by

$$\mathscr{A} = \frac{\Lambda_n\Gamma(n+1)}{p^{n+1}} \cdot \frac{e^{+qR}}{[pMc_f/(aR)](q + a + 1/R) + [H/(aR)](q + 1/R)}. \quad \text{(I-17)}$$

The subsequent calculations are carried out in a similar manner to those for the plane wall. The end result is equation (17).

APPENDIX II

Complementary error functions with complex arguments

The tables, reference [3], give values of the function,

$$w(z) = e^{-z^2}\left(1 + \frac{2j}{\sqrt{\pi}} \int_0^z e^{\zeta^2} d\zeta\right) \quad \text{(II-1)}$$

where

$$z = \theta + j\lambda \quad \text{(II-2)}$$

thus:

$$w(z) = U(\theta; \lambda) + jV(\theta; \lambda). \quad \text{(II-3)}$$

Tabulated values of U and V are given.

Now from (II-1),

$$w(jz) = e^{z^2}\left(1 - \frac{2}{\sqrt{\pi}}\int_0^z e^{-\zeta^2}\,d\zeta\right) = e^{z^2}\,\mathrm{erfc}\,z. \tag{II-4}$$

Thus from the tabulated values, erfc (z) may be obtained, taking θ as the imaginary variable and $-\lambda$ as the real variable. Also, symmetry with respect to the imaginary axis in the λ, θ plane implies the same in the U, V plane. Thus,

$$e^{z^2}\,\mathrm{erfc}\,z = U(\lambda;\theta) - jV(\lambda;\theta) \tag{II-5}$$

$$e^{\bar{z}^2}\,\mathrm{erfc}\,\bar{z} = U(\lambda;\theta) + jV(\lambda;\theta). \tag{II-6}$$

For the case discussed, the two roots, equation (4), are the two conjugate complex variables z and $\bar{z}$.

APPENDIX III

Asymptotic solutions

(a) *The plane wall case*

The asymptotic solutions corresponding to cases (a) through (d) of paragraph 2.3 of the paper are here investigated. These asymptotic solutions are of significance as they delimit the range of possible solutions in Figs. 1 and 2.

For *case* (a) ($S = 0$) a trivial identity is obtained from the general solution, implying no change in fluid temperature with time. In order to analyse *case* (b) ($a = \infty$), it is convenient to write (6) for $n = 0$ in terms of a characteristic time which does not include the constant a:

$$\frac{vKs}{A_0} = \frac{2}{\sqrt{\pi}}\tau^{1/2}e^{-x^2/4\kappa t} - (1+sx)\,\mathrm{erfc}\frac{x}{2\sqrt{(\kappa t)}} + \frac{1}{\eta_2-\eta_1}\left\{\eta_2^2 e^{\eta_1^2\tau/S^2+\eta_1 ax}\cdot\mathrm{erfc}\left[\eta_1\tau^{1/2}/S + \frac{x}{2\sqrt{(\kappa t)}}\right] - \eta_1^2 e^{\eta_2^2\tau/S^2+\eta_2 ax}\,\mathrm{erfc}\left[\eta_2\tau^{1/2}/S + \frac{x}{2\sqrt{(\kappa t)}}\right]\right\} \tag{III-1}$$

where $\tau = s^2\kappa t$. The limit for $S = 0$ involves the calculation of

$$\lim_{\xi\to\infty}(e^{\xi^2}\,\mathrm{erfc}\,\xi) = 0 \tag{III-2}$$

which is easily obtained by application of l'Hopital's rule. Thus for $S = 0$ (case b),

$$\frac{vKs}{A_0} = \frac{2}{\sqrt{\pi}}\tau^{1/2}e^{-x^2/4\kappa t} - (1+sx)\,\mathrm{erfc}\frac{x}{2\sqrt{(\kappa t)}} + e^{sx+\tau}\,\mathrm{erfc}\left(\frac{x}{2\sqrt{(\kappa t)}} + \tau^{1/2}\right). \tag{III-3}$$

The last equation is identical with the classical result ([1], p. 306, equation 12). Fluid temperature is obtained by setting $x = 0$ in (III-3).

Case (c) ($s = \infty$): it may be seen from (6), again limiting consideration to constant heat input ($n = 0$), that as $s \to \infty$,

$$\frac{vK}{A_0} = 2\sqrt{\left(\frac{\kappa t}{\pi}\right)}e^{-x^2/4\kappa t} - x\,\mathrm{erfc}\frac{x}{2\sqrt{(\kappa t)}}. \tag{III-4}$$

Equation (III-4) is again in agreement with the classical result ([1], p. 75, equation 7).

Case (d) ($a = 0$) corresponds to zero heat dissipation to the walls. After considerable manipulation the result $v \equiv 0$ is obtained from equation (III-1). Thus fluid temperature rises linearily with time, i.e.

$$\frac{uKs}{A_0} = \tau. \tag{III-5}$$

Cases (b) and (d) are represented by curves $S = 0$ and $S = \infty$ in Fig. 1 respectively, while case (c) is represented by the curve $S = \infty$ in Fig. 2.

(b) *The spherical case*

Only the non-trivial cases $a \to \infty$ and $s \to \infty$ are investigated here.

For $a \to \infty$ (zero contact resistance), one of the three roots of (18) increases without bounds. The limit for (17) becomes,

$$\frac{Kv}{A_0 R} = \frac{R}{r}\left\{\mathrm{erfc}\left(\frac{r-R}{2\sqrt{(\kappa t)}}\right) + \frac{\eta_1}{\eta_2-\eta_1}e^{\eta_2(r-R)+\eta_2^2\kappa t}\cdot\mathrm{erfc}\left[\frac{r-R}{2\sqrt{(\kappa t)}} + \eta_2\sqrt{(\kappa t)}\right] - \frac{\eta_2}{\eta_2-\eta_1}e^{\eta_1(r-R)+\eta_1^2\kappa t}\cdot\mathrm{erfc}\left[\frac{r-R}{2\sqrt{(\kappa t)}} + \eta_1\sqrt{(\kappa t)}\right]\right\}. \tag{III-6}$$

For $s \to \infty$ (zero fluid heat capacity) (20) gives as limiting value (4), p. 248 of reference [1].

Résumé—Une analyse est présentée du comportement en régime transitoire d'un reservoir contenant du fluide bien mélangé. Des solutions nouvelles données se rapportent à des modèles géometriques simples, en prenant cependant compte de la variation de l'enthalpie totale du fluide avec le temps, et de la résistance à la transmission de la chaleur par convection aux parois. Ainsi, les résultats font avancer la solution du problème en toute sa généralité. Les modèles géometriques subis à l'analyse sont la parois plane semi-infinie en contact avec du fluide bien mélangé, et la cavité sphérique dans un solide d'étendue infinie. La fourniture de la chaleur peut être soit à débit constant, soit à débit variable avec le temps.

Des représentations graphiques de validité générale et des tables numériques sont données pour le cas de la paroi plane et du débit de la chaleur constant.

Zusammenfassung—Eine Untersuchung der zeitabhängigen Temperaturänderung von intern beheizten Flüssigkeitsspeichern ist in der vorliegenden Arbeit wiedergegeben. Neue Lösungen für einfache geometrische Modelle, die immerhin den Wärmeinhalt der Flüssigkeit und den Konvektionswiderstand an den Wänden mit in Betracht nehmen, werden behandelt, als ein Schritt zur Lösung des allgemeineren Problems.

Die geometrische Modelle sind: die halbunendliche flache Wand in Berührung mit gut gemischter Flüssigkeit und der kugelförmige Hohlraum. Lösungen für Zeitabhängigen und Zeitunabhängigen Wärmestrom werden wiedergegeben.

Allgemeingültige graphische Darstellungen sowie Tabellen für den Fall der flachen Wand und Zeitunabhängiger Wärmezufuhr sind in der Arbeit enthalten.

Аннотация—В статье излагается исследование зависимых от времени изменений температуры в нагретых из-внутри сосудах наполненных жидкостью. Рассматриваются новые разрешения для простых геометрических моделей, причём учитывается теплоёмкотсь жидкости а также конвекционное сопротивление у стенок. Эти исследованкя приближают нас к разрешению вопроса в общей форме.

Рассматриваются две геометрические модели: одна из них это полу-безконечная плоская стенка в соприкосновении с хорошо смешанной жидкостью, другая это шарообразная полость. В статье представлены разрешения при зависимом, а также при независимом от времени, притоке тепла.

Приводятся общие графические изложения и численные таблицы для плоской стенки при постоянном притоке тепла.